Separation and Purification Technology 311 (2023) 122958

Contents lists available at ScienceDirect

Separation and Purification Technology

journal homepage: www.elsevier.com/locate/seppur

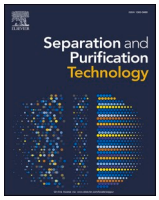

Intensified Nd extraction in small channels for NdFeB magnet recycling

Charlotte Pheasey, Panagiota Angeli *

ThAMeS Multiphase, Department of Chemical Engineering, UCL, Torrington Place, London WC1E 7JE, United Kingdom

ARTICLE INFO

Keywords:
Ionic liquids
Liquid-liquid
Rare earths
Mass transfer
Small channels

ABSTRACT

Neodymium (Nd) was continuously extracted from aqueous solutions by trioctylphosphine oxide (TOPO) dissolved in the ionic liquid 1-Butyl-3-methylimidazolium Bis (trifluoromethanesulfonyl)imide [C_4mim][Tf_2N] in small channel contactors. Kinetic studies confirmed a 1:6 Nd:TOPO extraction mechanism at high initial Nd concentrations of 0.005 and 0.01 M in a 0.001 M nitric acid aqueous phase. The continuous flow extractions were carried out in channels with 0.5 and 1 mm diameter and the effects of mixture velocity and residence time on the extraction efficiency and the mass transfer coefficient were investigated. At equal phase mixture velocities, the flow pattern studies highlighted a plug flow regime at mixture velocities of 0.01 to 0.05 m/s for both channels, resulting in interfacial areas of up to 4900 m^2/m^3 in the 0.5 mm channel and 2500 m^2/m^3 in the 1 mm channel. After 37.5 s residence time, extraction efficiencies of 80 % were found in the 0.5 mm channel at a $K_L\alpha$ of 0.09 s^{-1} and 70 % at 0.04 s^{-1} in the 1 mm channel. The same extraction efficiencies were achieved in 1–2 h in the batch systems.

1. Introduction

Rare earths are gaining global importance from an engineering and a geopolitical perspective. These elements form the basis of several green technologies such as batteries, hard drives, catalysts, and magnets. As economies decarbonise in line with the sustainable development goals, the use of these materials is set to increase almost exponentially [1]. Neodymium (Nd) is the element that makes up the largest proportion of this demand through the increasing use of Neodymium Iron Boron (NdFeB) magnets, predominantly in wind turbines. To meet the Paris climate agreement of net zero by 2050 [2] these renewable technologies will become increasingly necessary, putting a strain on the life cycle of rare earth elements.

The term *rare* is largely related to global imbalances in supply. 95 % of rare earth metals are sourced from China [3] where in addition, ores often contain low concentrations of the desired materials. This monopoly often results in unbalanced supply chains [4] that are unsustainable due to the mining practices used [5]. To meet increasing demand, supply chains require the additional input of recycled material to create more sustainable and stable resource streams. The recycling of NdFeB magnets is becoming a promising resource, with increased decommissioning creating substantial volumes of waste material [6].

Solvent extraction has been highlighted as the most effective technique for the recycling of NdFeB magnets and other similar materials [3,6–10]. It involves the interaction of two immiscible phases with mass transfer across the phase boundary. The two phases are the aqueous solution, usually acidic, in which the material to be recycled is dissolved, and an organic phase solvent which often contains an extractant molecule. Selection and adaptation of this organic phase determines the kinetics of extraction.

Evolution of solvent extraction has resulted in increased efficiencies and ever reducing carbon footprints. Traditionally organic solvents, such as heptane and kerosene formed the basis of the organic phase. This was adapted in time by the addition of or individual use of extractant ligands (e.g. D2EHPA and Cyanex 272) [8] facilitating changes in fluid properties and enhanced kinetics. These primary solutions based on organic solvents are, however, hindered by environmentally damaging characteristics and high hazard ratings. More recently, research has focused into utilising alternative solvents [11–15]. Hydrometallurgical metal extractions are beginning to utilise ionic liquids, IL, (salts with low melting points) more frequently due to their remarkable physicochemical properties including low volatility, high thermal and chemical stability, and low flammability. A key advantage of using ionic liquids is their high selectivity and specificity. In addition, high distribution coefficients and very high extraction efficiencies (up to 100 %) in fractions of the times of traditional solvents have been reported [12,16–20], making them highly appealing for industrial application.

The review by Wang et al. [16] highlights the imidazolium cations of

* Corresponding author.
E-mail address: p.angeli@ucl.ac.uk (P. Angeli).

https://doi.org/10.1016/j.seppur.2022.122958
Received 18 October 2022; Received in revised form 14 December 2022; Accepted 17 December 2022
Available online 20 December 2022

ionic liquids as the most effective for rare earth extractions due to their relatively low viscosity, ease of synthesis and affinity to the lanthanide elements. As the alkyl chain length of this cation increases extraction efficiencies have been found to decrease [21]; hence, the C_4mim cation is the most extensively used for rare earth extractions [20].

Short chain imidazolium cations display a mechanistic advantage over longer chain cations. The short chain results in a hydrophilic cation with an affinity to the aqueous phase, promoting exchange. As the chain lengthens, the cation becomes hydrophobic hindering the kinetically fast cation exchange mechanism, and hence, distribution coefficients reduce with increasing chain length at a given extractant concentration [21]. In addition to this mechanistic advantage, the low viscosity of shorter alkyl chain length cations also makes them preferable from a hydrodynamic stance. As the viscosity of an ionic liquid increases it has been shown to negatively affect hydrodynamics and subsequently extraction efficiencies in small channels [11,22]. The C_4mim cation is therefore the most utilised cation in small channel applications [19,23–25].

The extractants frequently used with organic solvents are the organophosphorus compounds Cyanex272, PC88A and DEHPA. With the IL as the extracting phase, however, neutral and acidic ligands such as TBP, TODGA, and Cyanex923 have been used more frequently [16]. Further improvements in extraction efficiency have been achieved with synergistic extractant combinations and functionalised ionic liquids that result in high selectivity to the desired material [9]. The range of combinations and functionalisation possible with IL makes for an interesting development in solvent extraction. The large range of options, however, means that a clear optimum combination has not been defined for Nd extractions. In addition, when utilising ionic liquids, the ions can partake in the mechanism altering the kinetics [13,15] in contrast to conventional solvents where the desired material binds to the extractant molecule. This phenomenon is of large interest in the field of hydrometallurgy as it gives further tuning capabilities for increased extraction efficiency.

Some recent examples of the use of ionic liquids for Nd extraction include studies by Asadollahzadeh et al. [26] who utilised the [C_6mim][NTf2] with TOPO and TBP over a supported liquid membrane achieving a maximum extraction efficiency of 90 % and that of Turanov et al. [27] who used the [C_4mim][Tf2N] with TODGA and TBP achieving maximum distribution coefficient, D, (Log(D) of 2).

Traditionally batch mixer-settler equipment has been used for solvent extraction. The high costs often associated with novel solvents and a need for increased process efficiency are driving process innovations. Recently, small channel contactors have been proposed as a means to intensify processes. Small channels offer a variety of benefits over traditional batch systems including small footprints, reduced material use, and increased mass transfer rates. They have been found to increase mass transfer coefficients by 1 – 2 orders of magnitude due to stable flow patterns, improved mixing, and large interfacial areas [24]. The recent use of small channels for metal extractions is summarised by Asrami et al. [11]. He et al. [28] used a serpentine microchannel for Nd extraction into an organic solvent and found that residence times reduced from 560 s to 12 s and separation factors increased from 2.19 to 2.23 compared to batch studies.

There is very limited work on the extraction of Nd in small channels, with the known studies limited to organic solvents [28,29]. This work for the first time investigates the combined effects of both ionic liquids and small channel processing on the extraction of Nd for a double process intensification of the solvent and the contactor. In what follows the kinetics of extraction are studied followed by continuous flow extractions in small channels. The effects of mixture velocity, residence time, channel diameter, metal: extractant ratio, and metal concentration are investigated in relation to extraction efficiency and mass transfer coefficient.

2. Materials, experimental setup and procedure

2.1. Materials

Neodymium (III) nitrate hexahydrate $Nd(NO_3)_3 \bullet 6H_2O$ (purity 99.9 % and a molecular weight 435.38 g/mol), the extractant trioctylphosphine oxide (TOPO) (purity 99 % molecular weight 386.63), and 1-Butyl-3-methylimidazolium Bis (trifluoromethanesulfonyl)imide, [C_4mim][Tf_2N] at 98 % purity grade (CAS number: 174899–83-3) were purchased from Sigma Aldrich and used as received. Table 1 summarises the physical properties of the fluids used. The viscosity of the ionic liquid before and after it was saturated with water was measured using a digital Rheometer DV-111 Ultra (Brookfield) (+ / −1%). The surface and interfacial tensions were measured with the pendant drop method using a DSA100E drop shape analyser (KRÜSS Scientific) (accuracy 0.3mN/M).

The ionic liquid and extractant system chosen in this work is based on literature findings, considering extraction efficiency, cost, applicability for small channel operation, and scalability. The hydrophobic ionic liquid, 1-Butyl-3-methylimidazolium Bis (trifluoromethanesulfonyl)imide, [C_4mim][Tf_2N] was chosen due to its relatively low viscosity and proven suitability for Nd extractions [9]. The anion is considered non-hazardous in comparison to other typical anions such as PF_6. Neutral extractants have been highlighted as the most effective for rare earth extractions [16] hence the trioctylphosphine oxide (TOPO) extractant was chosen as it is also cheap, easy to manufacture, and has previously been successfully implemented for Nd extractions [30]. The chosen system combines an IL and extractant that result in effective extraction and are low cost, low viscosity,

Table 1
Physical properties of the fluids used in experiments at room temperature (298K) and atmospheric pressure. (a) Average measured value, measurement error Viscosity +/- 0.8%, Density +/- 0.8%, Surface tension +/- 0.5%, and Interfacial tension +/- 0.5%. (b) Commercially provided.

Physical property	Pure [C_4mim][Tf_2N]	Water saturated [C_4mim][Tf_2N]	Water saturated [C_4mim][Tf_2N] + 0.3 M TOPO
Viscosity, μ, kg/ms	0.052 [a] 0.0614 [b]	0.041 [a]	0.052 [a]
Density, ρ, kg/ms^3	1420 [a] 1430 [b]	1390 [a]	1440 [a]
Surface tension, σ, N/m	0.0313 [a]	0.0316 [a]	0.0297 [a]
Interfacial tension, γ, N/m	0.0119 [a]	0.0118 [a]	0.0119 [a]

and easy to source.

2.2. Experimental setup and procedure

All experiments were carried out at room temperature (T = 298 K) and atmospheric pressure. The pH was constant for all experiments (pH = 3) and was checked using a pen-type pH meter (Velleman) with a 0.2 pH accuracy. Aqueous phase samples were analysed for Nd concentration by a MP-AES (Agilent 4210) at a wavelength of 814 nm. Samples were compared to a previously created calibration curve of known Nd concentrations (0 – 100 ppm) using a Neodymium standard solution of 1000 mg/L Nd in 70 % nitric acid purchased from Merck.

Solutions of the aqueous phase were created at 3 different nominal Nd concentrations. As the actual concentrations were slightly different than the nominal ones in what follows we denote with (a) the nominal and with (b) the actual which was an average over 3 experiments. The concentrations used were $0.005^{(a)}$ ($0.0058^{(b)}$), $0.01^{(a)}$ ($0.0093^{(b)}$), and $0.05^{(a)}$ ($0.056^{(b)}$) M. These were made by dissolving Neodymium (III) nitrate hexahydrate in a 0.001 M nitric acid solution. The organic phase was then created by dissolving a range of TOPO concentrations in the ionic liquid. Both phases were individually magnetically stirred until a homogenous mixture formed. As the IL is hydroscopic it was pre equilibrated with an equal volume of deionised water for 45 min and separated with a separation funnel prior to experiments.

The equilibrium studies and subsequent mechanism investigation were carried out as batch extraction experiments, 5 ml of each phase were brought into contact in a magnetically stirred sealed vessel. For the initial equilibrium studies investigating equilibration time, the vessel was left to mix for 16 h (960 min) and periodically removed from the stirrer plate for sampling, where, upon removal, a distinct interface formed. Equal volumes of both the aqueous phase (retained for further analysis) and the organic phase (discarded) were removed with a graduated pipette. This lasted around 1 min per sample and was assumed to have a negligible effect to the experiment. For the subsequent equilibrium and mechanism studies, samples were left to equilibrate for 4 h, and an aqueous phase sample was removed for analysis. The aqueous samples were analysed in the MP-AES for Nd concentration to calculate the Extraction percentage (Extraction%) and the Distribution Coefficient, (D), as follows.

$$\text{Extraction}\% = \left(\frac{\text{Nd}_{\text{initial}} - \text{Nd}_{\text{final}}}{\text{Nd}_{\text{initial}}}\right) \times 100 \quad (1)$$

$$D = \frac{\text{Nd}_{\text{initial}} - \text{Nd}_{\text{final}}}{\text{Nd}_{\text{initial}}} \quad (2)$$

The continuous small channel extraction setup can be seen in Fig. 1. Two high precision syringe pumps (K_d Scientific) were used to feed the two phases into the channel through a *T*-junction. Two different *T*-junctions were used with side channel internal diameters 0.5 mm and 1.34 mm respectively. The aqueous phase entered tangential to the main channel and the organic phase entered perpendicular to it (see Fig. 1). The main channels were hydrophobic PTFE capillaries, with diameters 0.5 and 1 mm. The flow patterns were observed using a Photron Fastcam-ultima high speed camera at frame rates between 1000 and 5000 Hz, depending on the flowrates. For the visualisation of the flow, a viewing box encompassed the channel which was filled with a glycerol/water mixture that matched the refractive index of the channel wall to minimise reflections. The viewing section was illuminated with a 60 W continuous arc lamp. Images were analysed using a MATLAB post processing routine to determine the characteristics of the different flow patterns. The length of the plugs were averaged over 10 images giving a standard deviation of 3 %, which confirms the uniformity of the flow.

All channel flow extractions were undertaken at equal phase flowrates between 0.059 and 0.294 ml/min (0.5 mm channel) and 0.236 – 1.18 ml/min (1 mm channel) equating to mixture velocities of 0.01 – 0.05 m/s. To study the effect of mixture velocity on the flow patterns and the extraction, a test section with length of 30 cm was chosen. To study the effect of residence time without affecting the flow patterns, different channel lengths were used, varying from 7.5 to 75 cm whilst the phase flowrates were kept constant. At the end of the channel, the mixture entered a membrane separator (Zaiput) fitted with a Hydrophilic PTFE IL-2000-S10 membrane that separated the aqueous and the organic phases. The aqueous phase samples were diluted to within 10–100 ppm and analysed by MP-AES to obtain the concentration of Nd.

3. Results and discussion

3.1. Equilibrium studies and mechanism of extraction

The aim of these investigations was to identify the equilibrium concentrations, the extraction kinetics, and the distribution coefficients for the Nd separation. The equilibrium studies and subsequent mechanism investigation were carried out as batch extraction experiments building on the kinetic evaluations made by Rout et al. and Yang et al. [21,30]. Both investigated multiple ionic liquids for initial Nd concentrations of 0.0007 and 0.0001 M respectively concluding that using $[C_4mim][Tf_2N]$ as the solvent resulted in the highest extraction efficiency. Experiments differed in the extractant used; Rout et al. [21] used Cyanex923 while Yang et al. [30] used TOPO. Even though these extractants exhibit high molecular similarity they were found to behave

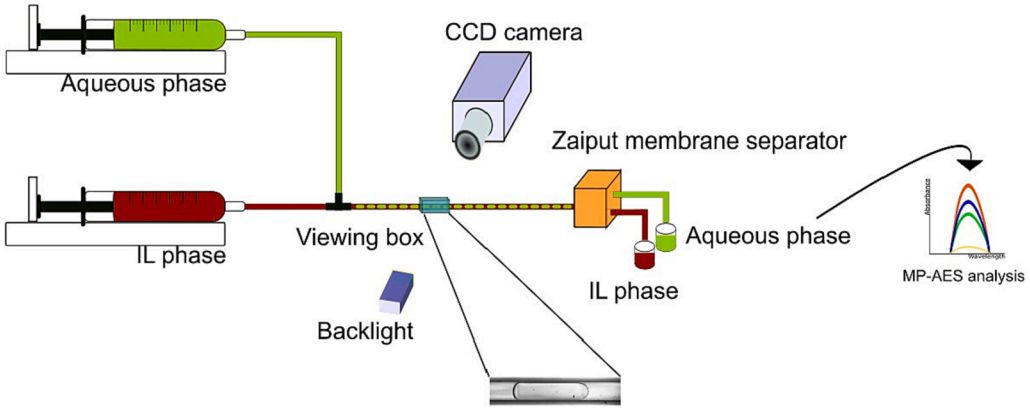

Fig. 1. Experimental setup of continuous solvent extraction in small channels.

differently in terms of kinetics. The present experiments build on this kinetic understanding. The [C_4mim][Tf_2N] solvent with the TOPO extractant is used here at higher initial Nd concentrations than in the previous studies. Mechanisms of extraction have been proven to change with a variety of system changes, including, initial metal concentration and hence the system change made here must be kinetically evaluated.

Ionic liquid extraction mechanisms can be cation exchange, anion exchange or neutral [9]. The mechanism largely depends on the hydrophobicity of the ionic liquid. The C_4mim cation used here is known to promote cation exchange. As the C_4min is a short hydrophilic alkyl chain, it is highly soluble in the aqueous phase and therefore favours exchange. When the Nd^{3+} ions are extracted into the ionic liquid phase by binding to the extractant, simultaneously the IL cations move into the aqueous phase for charge balance. Examples of the potential mechanisms for Nd extraction by [C_4mim][Tf_2N] as proposed by Rout et al. [21] are given below in equations (3a) to (3c), where Q represents the ionic liquid cation and L the extractant.

$$Nd^{3+}_{(aq)} + nL_{(org)} + (n)Q[Tf_2N]_{(org)} \leftrightarrow NdL_n(Tf_2N)_{n(org)} + (n)Q^{+}_{(aq)} \quad (3a)$$

$$[Nd(NO_3)_n]^{n+}_{(aq)} + nL_{(org)} + nQ[Tf_2N]_{(org)} \leftrightarrow NdL_n(NO_3)_n(Tf_2N)_{n(org)} + nQ^{+}_{(aq)} \quad (3b)$$

$$Nd^{3+}_{(aq)} + 3NO_3^{-}{}_{(aq)} + nL_{(org)} \leftrightarrow NdL_n(NO_3)_{3(org)} \quad (3c)$$

Rout et al. [21] investigated the use of the [C_4mim][Tf_2N] ionic liquid with the Cyanex923 extractant. The molecular structure of Cyanex923 is more than 90 % TOPO (Fig. 2) and the remaining 10 % consists of molecules with some variations in the alkyl chain length.

The mechanism suggested by Rout et al. [21] for [C_4mim][Tf_2N] with Cyanex923 can be seen in eq. (3a) where the number, n, of extractant molecules, L, is 3 (giving a metal: extractant ratio of 1:3). By altering the nitrate and cation concentrations Rout et al. [21] concluded that no nitrate ions were involved in the mechanism and 3 cation molecules (Q) of the ionic liquid were exchanged.

Based on the molecular similarity for TOPO and Cyanex923 it may be assumed that the mechanisms of extraction will be the same. However, Yang et al. [30] previously proposed a similar mechanism to that of Rout et al. [21], but with a 1:6 of metal: extractant ratio.

The above two studies used high excess extractant concentrations 14 – 300 M and 100–350 M and low initial Nd concentrations, 0.0007 and 0.0001 M, respectively. In contrast extractant concentrations of 0.015 – 2.5 M were investigated here at initial Nd concentration of 0.005 – 0.05 M in line with those seen in NdFeB magnets.

The change in Nd concentration in the aqueous phase from an initial Nd concentration of 0.005 M[(a)] (0.0058[(b)]) over 960 min can be seen in Fig. 3. It was found that equilibrium is reached in 240 min for all Nd: TOPO ratios apart from ratio equal to 30, where it is reached in 30 min due to near 100 % extraction percentage being reached. As the metal concentration increases the ratio at which 100 % extraction occurs decreases.

The distribution coefficient (equation (2)) obtained at a range of TOPO and metal concentrations is shown in Fig. 4. As it can be seen Log (D) increases with increasing Log (TOPO) reaching a maximum at above 3 for all initial Nd concentrations. This is above the values found by Rout et al. [21] where a maximum Log(D) of 1 was measured. At high TOPO concentrations, the distribution coefficient reaches a plateau for all metal concentrations. This plateau occurs due to 100 % extraction being reached in the system and hence an increase of the extractant results in no further increase in extraction. As the metal concentration increases, the metal: extractant ratio where this plateau is reached decreases. For 0.005 M[(a)] (0.0058[(b)]) initial Nd concentration, the plateau is reached at metal: extractant ratio of 30 (Log(TOPO) −1.02), for 0.01 M[(a)] (0.0093[(b)]) Nd at ratio equal to 12 (Log(TOPO) −0.92) and for 0.05 M[(a)] (0.056[(b)]) Nd at ratio equal to 9 (Log TOPO −0.35) (Fig. 4).

From Fig. 4 the relationship between Log(D) and Log(TOPO) is seen to form two distinct regions, a linear increase followed by a plateau. For the evaluation of kinetics, the linear increase region only was considered, to exclude extractant saturation effects. The results for initial Nd concentration of 0.05 M were not used as the maximum workable TOPO

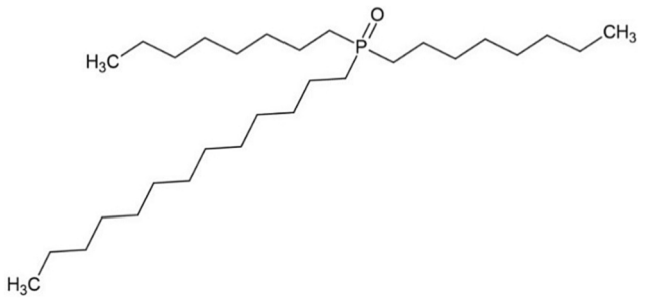

Fig. 2. Chemical structure of trioctylphosphine oxide (TOPO) extractant used in experiments.

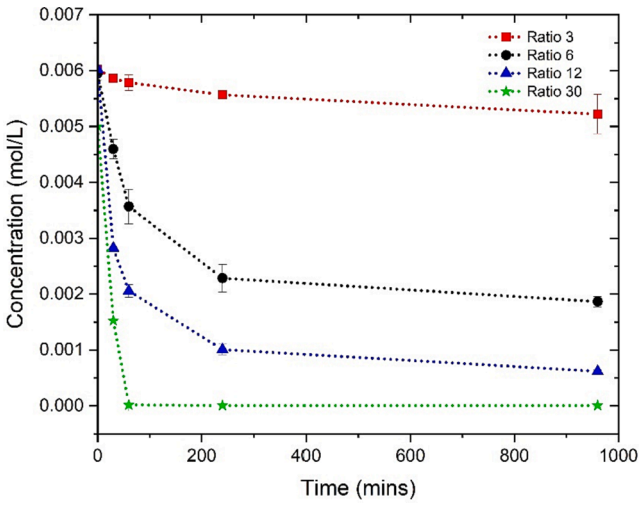

Fig. 3. Change in Nd concentration over a 16 h period from an initial Nd concentration 0.005 M[(a)] (0.0058[(b)]) and initial Nd:TOPO of 3,6,12, and 30.

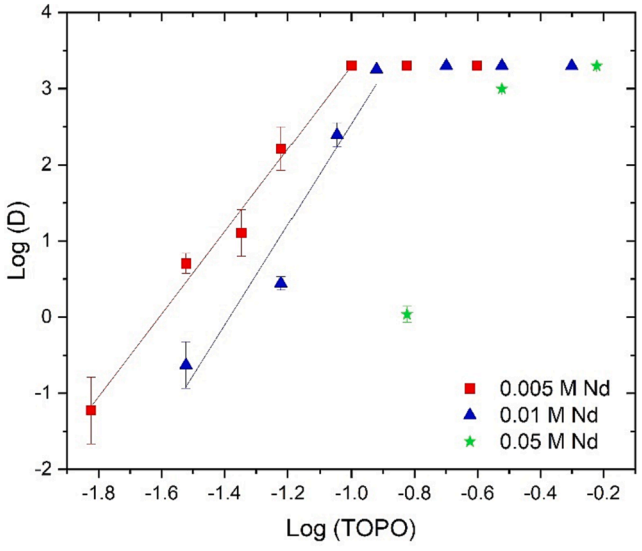

Fig. 4. Effect of TOPO concentration on the distribution coefficient of Nd into [C_4mim][Tf2N] at initial Nd concentrations (0.005, 0.01 and 0.05 M).

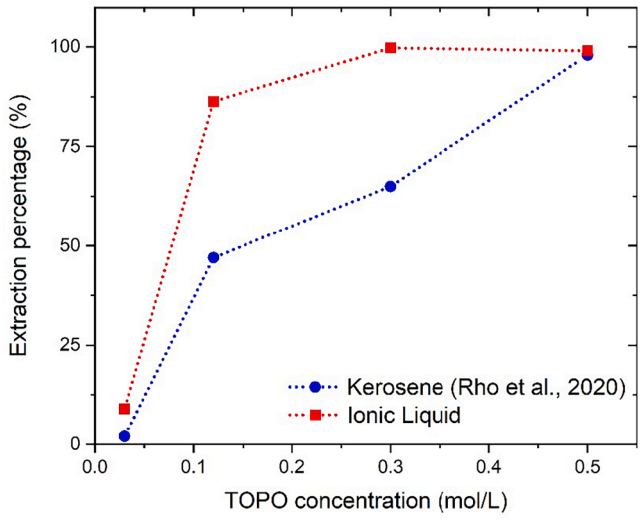

Fig. 5. Nd extraction after 30 min at a range of TOPO concentrations into Kerosene (Rho et al., 2020) and into [C_4mim][Tf2N] for the current work. Initial Nd concentration 0.01 M.

solubility in the ionic liquid is 0.6 M, above which TOPO cannot be dissolved within a 3 h time frame. The slopes of the lines for the 0.005 M and 0.01 M initial Nd concentration are 5.45 and 6.03 respectively. This indicates that every Nd element binds to 6 TOPO molecules upon extraction, in agreement with the mechanism proposed by Yang et al. [30]. The results show that the higher Nd concentrations used here have not resulted in any kinetic changes. These studies confirm the kinetic difference of TOPO to Cyanex923 in [C_4mim][Tf_2N].

Yang et al. [30] found maximum extraction percentages of 80 % at a Nd:TOPO ratio of 1:350, whereas in the current study similar extraction percentages are achieved at a 1:5 ratio only. Rho et al. [31] investigated extractions using the same extractant and initial Nd concentrations as those here but with kerosene as the organic solvent. The extraction percentage is plotted in Fig. 5 together with the results from the current work. As can be seen, utilising the ionic liquid gave a 45 % increase in extraction percentage at a given extractant concentration. This is despite the more favourable extraction kinetics with kerosene (metal: extractant ratio of 1:3) than with the ionic liquid (metal: extractant ratio of 1:6). This increase in extraction percentage with the ionic liquid highlights the effectiveness of the cation exchange mechanism over traditional solvent mechanisms.

The results of these studies establish an effective organic phase combination of the TOPO extractant with the [C_4mim][Tf_2N] ionic liquid for Nd extractions for high metal loadings and low extractant concentrations.

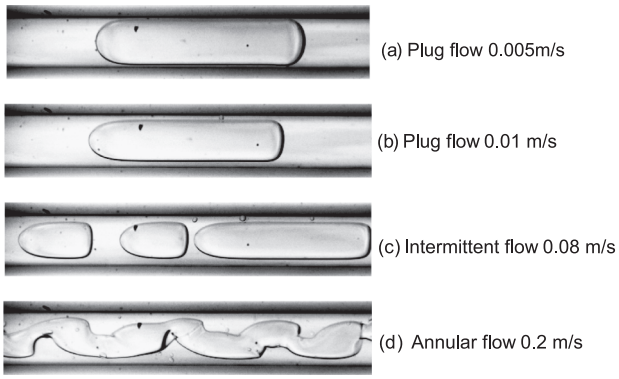

Fig. 6. (a-d) - Changes in flow pattern with increasing mixture velocity at equal phase flowrates in a 1 mm microchannel. Ionic liquid makes up the continuous/slug and aqueous phase makes up the dispersed/plug.

3.2. *Continuous flow extractions hydrodynamics.*

The flow patterns of the two immiscible liquids in small channels directly affect mixing and interfacial area and thus mass transfer [32,33]. For the liquids and materials used here a flow pattern map was developed previously by Phakoukaki et al. [23]. Flow patterns include plug, drop, intermittent, annular, and dispersed flow depending on the phase volumetric flowrates.

Plug flow (see Fig. 6) is the preferable flow pattern for mass transfer between two liquid phases in small channel contactors [34]. It has high interfacial area to volume ratio, which for processes involving transfer of material between two phases, increases the contact between the phases and the mass transfer. In addition, circulation patterns develop inside the plugs and slugs which improve radial mixing transferring material closer to the interfaces, thus increasing the concentration gradient and improving mass transfer [32]. Finally, in plug flow there is a thin film of the continuous phase forming between the dispersed plugs and the channel wall, where mass transfer is very fast due to the short diffusion distance [35]. The combination of large interfacial areas, improved radial mixing, and thin films provide preferable conditions for mass transfer.

In the current studies, the Bond numbers ($Bo = \Delta\rho g D^2/\gamma$) for the 0.5 and 1 mm channels are 0.88 and 0.34 respectively, indicating that gravitational forces are not significant, and the plug flow will be symmetric. In addition, Reynolds numbers ($Re = \rho_{mix} d U_{mix}/\mu_{mix}$) range from 0.034 to 10.2 (0.001 – 0.3 m/s) for the 1 mm channel and from 0.017 to 5.09 (0.001 – 0.3 m/s) for the 0.5 mm channel, indicating that inertial forces are small. The flow patterns are, therefore, dominated by capillary forces leading to the formation of stable plug flow [36] as shown in Fig. 6 (a,b). As flowrate increases, the inertial forces increase initiating instabilities [34] as can be seen in Fig. 6 (c,d). This flow transition occurs for capillary numbers ($Ca = \mu U_{mix}/\sigma$) equal to 0.8 for the 0.5 mm channel and 0.3 for the 1 mm channel respectively [23]. The capillary number for the departure from plug flow decreases with increasing channel diameter, as the significance of inertial forces increases with channel diameter. Based on these, we chose flowrates of 0.01 – 0.05 m/s for the extraction experiments to maintain a uniform plug flow.

At low flowrates plugs are symmetrical along the centre axis while their ends are almost hemispherical caps. As the flowrates increase, the

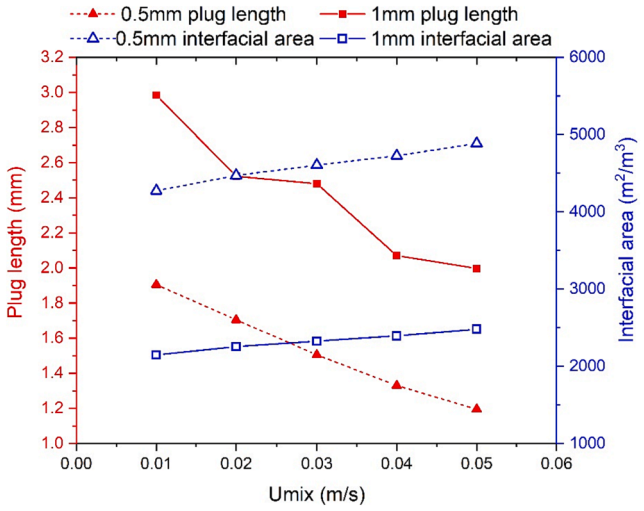

Fig. 7. Changes in the measured plug length (mm) and calculated interfacial area (m^2/m^3) with mixture velocity m/s in a 0.5 mm and 1 mm ID channel.

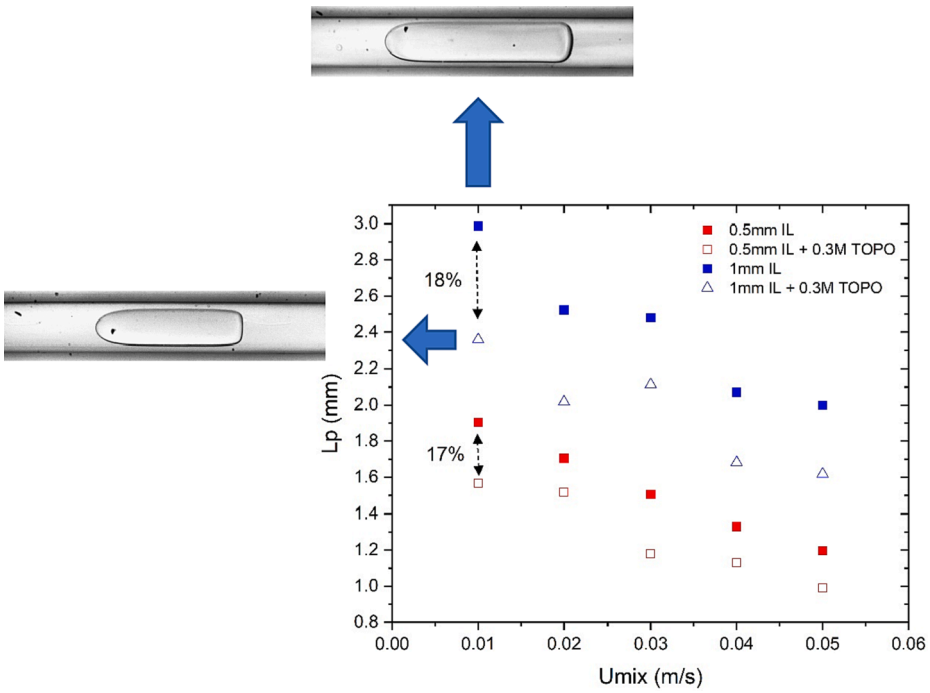

Fig. 8. Changes in the measured plug length (mm) with increasing mixture velocity in a 0.5 and 1 mm channel ID length 30 cm. Plug lengths measured for a [C_4mim][Tf2N] organic phase and a [C_4mim][Tf2N] + 0.3 M TOPO organic phase.

plug lengths reduce, the thickness of the film surrounding them increases, while the front of the plug acquires a bullet shape, and the back flattens. These changes affect the interfacial area available for mass transfer. The specific interfacial area can be calculated from the plug length and the film thickness for a unit cell of one plug and one slug as follows [23]:

$$\alpha_p = \frac{6L_p}{3w_pL_p - {w_p}^2} \tag{11}$$

Plug lengths (L_p) were obtained experimentally and are shown in Fig. 7. For the film thickness the following correlation was used $\frac{b}{R} = 0.643(3Ca)^{2/3}/1 + 0.643x2.5(3Ca)^{2/3}$ [35] applicable for Ca ranging from 0.0001 to 1 as accurate measurements of film thickness could not be made with the current imaging set up. As can be seen in Fig. 7 the interfacial area increased with mixture velocity from 4300 to 4900 m^2/m^3 for the 0.5 mm channel. These values far exceed those found in the standard equipment of a mixer settler where maximum interfacial areas of 1000 m^2/m^3 have been reported [37].

The addition of the extractant to the ionic liquid phase alters the viscosity. For the maximum batch extractant concentration used here of 0.3 M, the viscosity of the ionic liquid phase changes from 0.041 kg/ms to 0.051 kg/ms. To investigate the effects of the increased viscosity on the characteristics of the plug flow, further experiments were carried out with 0.3 M TOPO in the IL phase. The changes in the plug length can be seen in Fig. 8. There was a decrease in plug length of an average of 17 % with increased viscosity corresponding to a 4 % increase in interfacial area. It is therefore expected that an addition of 0.12 M of TOPO (extractant concentration used during channel extraction studies) would cause a plug length decrease of an average of 6.5 % resulting in a negligible increase of 1 % in interfacial area.

3.3. Channel extraction

Following the results of the equilibrium experiments, continuous flow extractions were investigated in the small channels with 0.01 M Nd in the aqueous phase and 0.12 M TOPO in the ionic liquid phase. The effects of both mixture velocity and residence time were investigated within the plug flow regime. The results were analysed for extraction efficiency (E%), Equation (13), which compares the extraction achieved to the maximum extraction reached at equilibrium, and the overall volumetric mass transfer coefficient ($K_L\alpha$), given by Equation (14).

$$E\% = \frac{C_{aq,in} - C_{aq,out}}{C_{aq,eq} - C_{aq,fin}} \times 100 \tag{13}$$

$$K_L\alpha = \frac{1}{\tau}\ln\left(\frac{C_{aq,eq} - C_{aq,in}}{C_{aq,eq} - C_{aq,fin}}\right) \tag{14}$$

3.3.1. Effect of mixture velocity

To investigate the effects of mixture velocity, the channel length was varied to maintain the residence time at 15 s across experiments. The results regarding extraction efficiency and mass transfer coefficient can be seen in Figs. 9 and 10 respectively.

For both channels there is an increase in extraction efficiency of 40 % and an increase in $K_L\alpha$ of 50 % as the mixture velocity increases from 0.01 m/s to 0.05 m/s. As Umix increases plug length decreases and film thickness increases leading to increased interfacial area (see Fig. 7). In addition, the internal mixing in the plugs also increases both with reduced plug length and increased mixture velocity [29], which further improves mass transfer. This combination of increased interfacial area and mixing result in the increase in extraction efficiency and mass transfer as seen in Figs. 9 and 10. The increase is, however, not linear and there is a distinct plateau after 0.02 m/s, while in the 1 mm channel a decrease is also seen at the highest mixture velocity used. The linear increase in interfacial area of 600 m^2/m^3 between 0.01 and 0.05 m/s for both the 0.5 and 1 mm channel (Fig. 7) has not resulted in a linear increase in extraction. It is possible that the plateau in extraction efficiency is linked to the mixing patterns within the plugs at high mixture velocities. Zhang et al. [29] showed that in an aqueous/ionic liquid system at equal phase flowrates and high mixture velocities an increase in mixture velocity broadly results in increased circulation and hence increased mixing and mass transfer, however a straightforward correlation between Umix and circulation time was not clear. According to the authors, the circulation time is a complex function which depended not only on the mixture velocity but also on the presence of stagnation

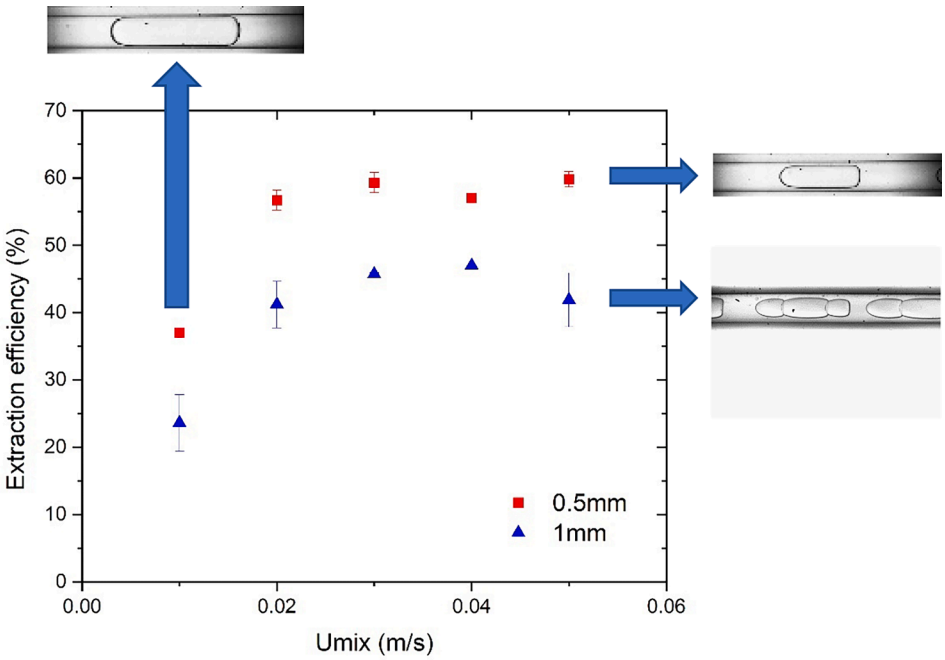

Fig. 9. Effect of increasing mixture velocity (0.01 – 0.05 m/s) at a constant residence time (15 s) on extraction efficiency in a 0.5 and 1 mm channel.

points and on film thickness. Tsaoulidis et al. [36] also showed that film thickness directly affects the presence or absence of secondary circulations. Although increases in Umix have resulted in increases in extraction, it is assumed that increases in film thickness have altered mixing patterns hindering a linear positive correlation with extraction efficiency.

Extraction efficiencies are consistently about 25 % higher in the 0.5 mm channel than in the 1 mm channel for most mixture velocities and additionally there is a 35 % increase in $K_L\alpha$ in the 0.5 mm channel compared to the 1 mm one. At a given mixture velocity plugs are shorter in the small channel, resulting in an interfacial area increase of about 100 % (Fig. 7). At 0.05 m/s, however, the extraction efficiency and $K_L\alpha$ in the 1 mm channel begin to decrease and the differences between the two channels increases. In the 1 mm channel, the 0.05 m/s mixture velocity is the boundary for the onset of unstable flows (see Fig. 6 and Fig. 9). In this regime, hydrodynamics become unstable, and the intermittent flow pattern establishes. As can be seen in Fig. 6c the intermittent flow regime is characterised by plugs and slugs of non-uniform lengths with some lengthened plugs. Long plugs lead to reduced interfacial area compared to the uniform plug flow (Fig. 6a and b). This interfacial area reduction will affect mass transfer and decrease the extraction efficiency and the $K_L\alpha$ as shown in Figs. 9 and 10. This highlights the superior nature of stable, uniform plug flow for mass transfer.

3.3.2. *Effect of residence time*

To investigate the effect of residence time on extraction, the mixture velocity was maintained at 0.02 m/s. Different residence times were obtained by changing the channel length. The results for extraction efficiency and mass transfer coefficients are shown in Figs. 11 and 12 respectively.

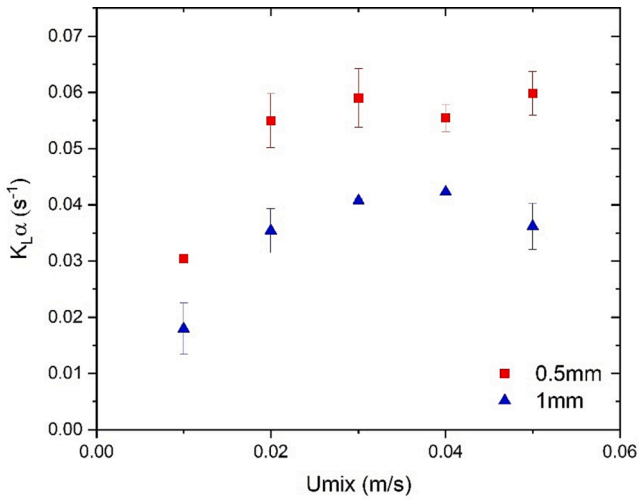

Fig. 10. Effect of mixture velocity increase (0.01–0.05 m/s) at constant residence time of 15 s on the volumetric mass transfer ($K_L\alpha$) in 0.5 and 1 mm ID channel.

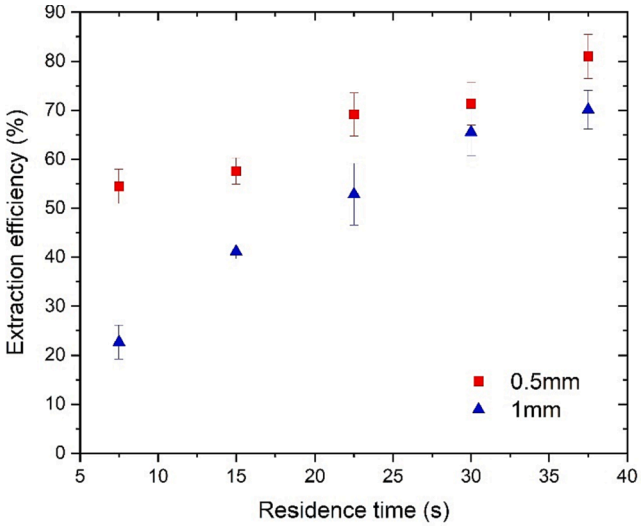

Fig. 11. Effect of increasing residence time (7.5 – 37.5 s) by increasing channel length (15–75 cm) at a constant mixture velocity of 0.02 m/s on the extraction efficiency in a 0.5 and 1 mm channel.

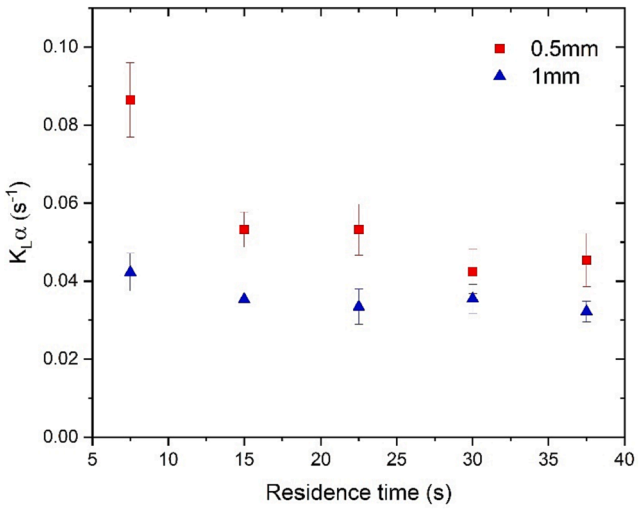

Fig. 12. Effect of increasing residence time (7.5 – 37.5 s) by increasing channel length (15–75 cm) at a constant mixture velocity of 0.02 m/s on the volumetric mass transfer ($K_L\alpha$) in a 0.5 and 1 mm channel.

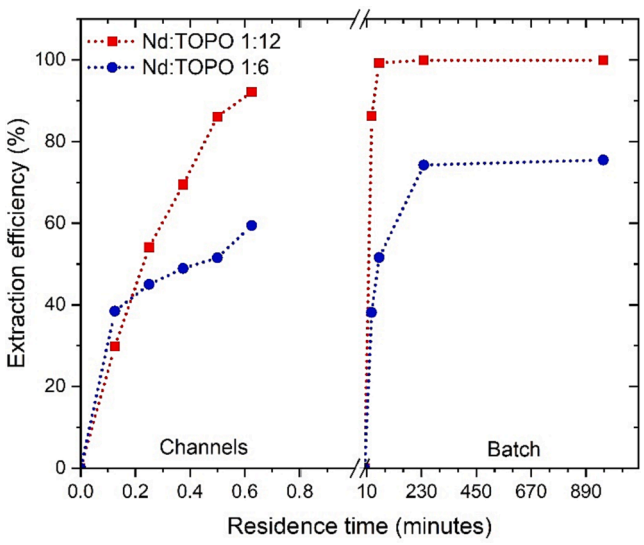

Fig. 13. Batch vs Channel extraction efficiency over time for initial Nd conc 0.01 M at Nd:TOPO ratios of 6 and 12.

As can be seen from Fig. 11, there is an increase in extraction efficiency between residence times 7.5 and 37.5 s in both channels. An increase in residence time results in increased contact time of the phases, facilitating increased mass transfer. This increase is more significant in the 1 mm channel at 50 % compared to the 25 % increase for the 0.5 mm channel. This is due to the initially high extraction efficiencies in the 0.5 mm channel already achieved by 7.5 s.

Overall, the extraction efficiencies are higher in the 0.5 mm channel than in the 1 mm. The smaller and more frequent plugs in the 0.5 mm channel compared to the 1 mm result in significantly higher interfacial areas (Fig. 7) and hence favour fast mass transfer. This difference however is not uniform; it is larger at short residence times compared to the long ones due to the difference in the mixing zone effects between the two channels. At a residence time of 15 s the extraction efficiency in the 0.5 mm channel is 30 % higher than in the 1 mm one, while at 37.5 s the difference is less than 10 %. The mixing zone is known to facilitate increased mass transfer due to the increased fluid interactions and high concentration gradients in this region [33]. The high extraction efficiency in the 0.5 mm channel at low residence time compared to the 1mm channel indicates that in the 0.5 mm channel mixing at the inlet is more efficient. As the residence time increases, extraction tends to equilibrium and this zone makes up a smaller proportion of the total system resulting in reduced differences between the two channels.

The difference in mass transfer between the two channels is further highlighted in the mass transfer coefficient results (Fig. 12). In the 0.5 mm channel, $K_L\alpha$ decreases initially with residence time but after 15 s it remains almost constant. In the large channel, the mass transfer coefficient only slightly decreases initially, while after a residence time of 15 s it remains almost constant. The *T*-junction inlet mixing zone is the point of increased mass transfer in the system. At short residence times (short channel length) this makes up a significant portion of the total system and hence $K_L\alpha$ is highest for low residence times. As the residence time increases (long channel lengths) the mixing zone is only a small proportion of the total system and plug flow becomes well established resulting in a plateau in the mass transfer coefficient. The greater decrease in $K_L\alpha$ seen in the 0.5 mm channel compared to the 1 mm channel highlights the increased effect of the mixing zone as the channel diameter decreases. At short residence times, small channels have better mass transfer performance compared to large channels.

Extraction efficiency reaches almost 80 % in 37.5 s in the 0.5 mm channel while it reaches 70 % in the 1 mm channel. These times are significantly lower than those of traditional mixer settlers [11]. Based on linear extrapolation of the data it is expected that both channels will have reached close to 100 % extraction efficiency within 60 s.

4. Conclusions

A double process intensification of the solvent extraction of Nd with ionic liquids in small channel contactors is demonstrated for the first time at Nd concentrations 0.005 – 0.05 M relevant to NdFeB magnets. Kinetic studies showed that the extraction mechanism is 1:6 Nd:TOPO in line with Yang et al. [30]. A 45 % increase in extraction percentage was seen compared to the use of TOPO in kerosene (Fig. 3).

Continuous flow extractions were carried out in the plug flow regime in 0.5 mm and 1 mm diameter channels where the aqueous solution formed the dispersed phase (plugs), and the ionic liquid solution formed the continuous phase (slugs). High extraction efficiencies were seen at low residence times with a linear increase in extraction efficiency of 45 % to 80 % for residence times 7.5 to 37.5 s in the 0.5 mm channel and of 22 % to 70 % in the 1 mm channel; for the same extraction efficiencies 1 h is required in the batch experiments (Fig. 13). For constant residence time, both the extraction efficiency and the mass transfer coefficient increased initially with mixture velocity, until they reached a plateau after 0.03 m/s (Figs. 9 and 10); this was attributed to a change in the mixing patterns in the plugs. For the 1 mm channel at the highest mixture velocity there was a decrease in the extraction efficiency and the $K_L\alpha$ when the pattern changed from stable plug to intermittent flow.

With increasing residence time at constant mixture velocity, the mass transfer coefficient decreased initially in both channels and then it reached a plateau, indicating that the mixing at the inlet has a large effect on mass transfer.

The mass transfer coefficients ranged from 0.05 to 0.1 s^{-1} in the two channels and are attributed to the large interfacial areas present in plug flow which reached 4900 m^2/m^3 in the 0.5 mm channel and 2500 m^2/m^3 in the 1 mm channel. The mass transfer coefficients initially increased with Umix, because of the better mixing and the decrease in plug length with increased velocity. $K_L\alpha$ reduced with residence time until a plateau was reached, highlighting the significant effect of the mixing at the inlet on mass transfer.

The results demonstrate the effectiveness of small channel flow extraction of Nd using ionic liquids as the solvent. Future work will investigate the mixing patterns inside the plugs to enable the prediction of mass transfer at different mixture velocities. It is important to note that scalability of IL extractions relies on further cost reductions using IL

recycling, which will be investigated in future studies. The hydrodynamic, kinetic and channel extraction findings can be used to inform future investigations into the recycling of NdFeB magnets.

CRediT authorship contribution statement

Charlotte Pheasey: Conceptualization, Methodology, Investigation, Writing – original draft. **Panagiota Angeli:** Conceptualization, Supervision, Writing – review & editing.

Declaration of Competing Interest

The authors declare that they have no known competing financial interests or personal relationships that could have appeared to influence the work reported in this paper.

Data availability

Data will be made available on request.

Acknowledgements

C. Pheasey would like to thank the Department of Chemical Engineering, UCL for their studentship.

References

[1] Y. Yang, A. Walton, R. Sheridan, K. Güth, R. Gauß, O. Gutfleisch, M. Buchert, B. M. Steenari, T. van Gerven, P.T. Jones, K. Binnemans, REE Recovery from End-of-Life NdFeB Permanent Magnet Scrap: A Critical Review, J. Sustainable Metall. 3 (2017) 122–149, https://doi.org/10.1007/s40831-016-0090-4.
[2] S. Teske, Achieving the Paris Climate Agreement Goals, Achieving the Paris Climate Agreement Goals: Global and Regional 100% Renewable Energy Scenarios with Non-Energy GHG Pathways for +1.5C and +2C. (2019) 491. 10.1007/978-3-030-05843-2.
[3] F. Xie, T.A. Zhang, D. Dreisinger, F. Doyle, A critical review on solvent extraction of rare earths from aqueous solutions, Miner. Eng. 56 (2014) 10–28, https://doi.org/10.1016/j.mineng.2013.10.021.
[4] K. Binnemans, P.T. Jones, Rare Earths and the Balance Problem, J. Sustainable Metall. 1 (2015) 29–38, https://doi.org/10.1007/s40831-014-0005-1.
[5] R. Ganguli, D.R. Cook, Rare earths: A review of the landscape, MRS Energy Sustainability 5 (2018) 1–16, https://doi.org/10.1557/MRE.2018.7.
[6] K. Binnemans, P.T. Jones, B. Blanpain, T. van Gerven, Y. Yang, A. Walton, M. Buchert, Recycling of rare earths: a critical review, J. Clean Prod. 51 (2013) 1–22, https://doi.org/10.1016/J.JCLEPRO.2012.12.037.
[7] M. Sethurajan, E.D. van Hullebusch, D. Fontana, A. Akcil, H. Deveci, B. Batinic, J. P. Leal, T.A. Gasche, M.A. Kucuker, K. Kuchta, I.F.F. Neto, H.M.V.M. Soares, A. Chmielarz, Recent advances on hydrometallurgical recovery of critical and precious elements from end of life electronic wastes - a review, Environ.. Sci. Technol. 49 (2019) 212–275, https://doi.org/10.1080/10643389.2018.1540760.
[8] N.N. Hidayah, Z. Abidin, The evolution of mineral processing in extraction of rare earth elements using liquid-liquid extraction: A review, Miner. Eng. 121 (2018) 146–157, https://doi.org/10.1016/j.mineng.2018.03.018.
[9] Y. Zhang, F. Gu, Z. Su, S. Liu, C. Anderson, T. Jiang, Hydrometallurgical Recovery of Rare Earth Elements from NdFeB Permanent Magnet Scrap: A Review, Adv. Mineral Process. Hydrometall. 10 (2020) 841, https://doi.org/10.3390/met10060841.
[10] A. Kumari, M.K. Sinha, S. Pramanik, S. Kumar Sahu, Recovery of rare earths from spent NdFeB magnets of wind turbine: Leaching and kinetic aspects, Waste Magnet. 75 (2018) 486–498, https://doi.org/10.1016/j.wasman.2018.01.033.
[11] M.R. Asrami, N.N. Tran, K.D.P. Nigam, V. Hessel, Solvent extraction of metals: Role of ionic liquids and microfluidics, Sep. Purif. Technol. 262 (2021), 118289, https://doi.org/10.1016/j.seppur.2020.118289.
[12] Y. Baba, F. Kubota, N. Kamiya, M. Goto, Recent Advances in Extraction and Separation of Rare-Earth Metals Using Ionic Liquids, J. Chem. Eng. Jpn. 44 (2011) 679–685, https://doi.org/10.1252/jcej.10we279.
[13] I. Billard, A. Ouadi, C. Gaillard, Liquid-liquid extraction of actinides, lanthanides, and fission products by use of ionic liquids: from discovery to understanding, Anal. Bioanal. Chem. 400 (2011) 1555–1566, https://doi.org/10.1007/s00216-010-4478-x.
[14] J. Park, Y. Jung, P. Kusumah, J. Lee, K. Kwon, C.K. Lee, Application of ionic liquids in hydrometallurgy, Int. J. Mol. Sci. 15 (2014) 15320–15343, https://doi.org/10.3390/ijms150915320.
[15] Y. Xiong, W. Kuang, J. Zhao, H. Liu, Ionic liquid-based synergistic extraction of rare earths nitrates without diluent: Typical ion-association mechanism, Sep. Purif. Technol. 179 (2017) 349–356, https://doi.org/10.1016/j.seppur.2017.02.026.
[16] K. Wang, H. Adidharma, M. Radosz, P. Wan, X. Xu, C.K. Russell, H. Tian, M. Fan, J. Yu, Recovery of rare earth elements with ionic liquids, Green Chem. 19 (2017) 4469, https://doi.org/10.1039/c7gc02141k.
[17] R. AliAkbari, Y. Marfavi, E. Kowsari, S. Ramakrishna, Recent Studies on Ionic Liquids in Metal Recovery from E-Waste and Secondary Sources by Liquid-Liquid Extraction and Electrodeposition: a Review, Mater. Circular Econ. 2 (2020) 1–27, https://doi.org/10.1007/S42824-020-00010-2.
[18] A. Rout, K. Binnemans, Liquid–liquid extraction of europium(III) and other trivalent rare-earth ions using a non-fluorinated functionalized ionic liquid, Dalton Trans. 43 (2014) 1862, https://doi.org/10.1039/c3dt52285g.
[19] Q. Li, P. Angeli, Intensified Eu(III) extraction using ionic liquids in small channels, Chem. Eng. Sci. 143 (2016) 276–286, https://doi.org/10.1016/j.ces.2016.01.004.
[20] S. Riaño, K. Binnemans, Extraction and separation of neodymium and dysprosium from used NdFeB magnets: an application of ionic liquids in solvent extraction towards the recycling of magnets, Green Chem. 17 (2015) 2931–2942, https://doi.org/10.1039/C5GC00230C.
[21] A. Rout, K. Binnemans, Influence of the ionic liquid cation on the solvent extraction of trivalent rare-earth ions by mixtures of Cyanex 923 and ionic liquids, Dalton Trans. 44 (2015) 1379, https://doi.org/10.1039/c4dt02766c.
[22] W. Vereycken, J. van Stee, S. Riaño, T. van Gerven, K. Binnemans, Non-equilibrium solvent extraction in milliflow reactors: Precious and base metal separations with undiluted ionic liquids, Sep. Purif. Technol. 265 (2021), 118490, https://doi.org/10.1016/j.seppur.2021.118490.
[23] Y.-V. Phakoukaki, P. O'Shaughnessy, P. Angeli, Intensified liquid-liquid extraction of biomolecules using ionic liquids in small channels, Sep. Purif. Technol. 282 (2022), 120063, https://doi.org/10.1016/J.SEPPUR.2021.120063.
[24] D. Tsaoulidis, V. Dore, P. Angeli, N.V. Plechkova, K.R. Seddon, Flow patterns and pressure drop of ionic liquid–water two-phase flows in microchannels, Int. J. Multiph. Flow 54 (2013) 1–10.
[25] D. Tsaoulidis, V. Dore, P. Angeli, N.V. Plechkova, K.R. Seddon, Extraction of dioxouranium(VI) in small channels using ionic liquids, Chem. Eng. Res. Des. 91 (4) (2013) 681–687.
[26] M. Asadollahzadeh, R. Torkaman, M. Torab-Mostaedi, A. Hemmati, A. Ghaemi, Efficient recovery of neodymium and praseodymium from NdFeB magnet-leaching phase with and without ionic liquid as a carrier in the supported liquid membrane, Chem. Pap. 74 (12) (2020) 4193–4201.
[27] A.N. Turanov, V.K. Karandashev, M. Boltoeva, Solvent extraction of intra-lanthanides using a mixture of TBP and TODGA in ionic liquid, Hydrometall. 195 (2020), 105367, https://doi.org/10.1016/J.HYDROMET.2020.105367.
[28] Y. He, K. Chen, C. Srinivasakannan, S. Li, S. Yin, J. Peng, S. Guo, L. Zhang, Intensified extraction and separation Pr (III)/Nd (III) from chloride solution in presence of a complexing agent using a serpentine microreactor, Chem. Eng. J. 354 (2018) 1068–1074, https://doi.org/10.1016/j.cej.2018.07.193.
[29] L. Zhang, F. Xie, S. Li, S. Yin, J. Peng, S. Ju, Solvent extraction of Nd(III) in a y type microchannel with 2-ethylhexyl phosphoric acid-2-ethylhexyl ester, Green Process. Synth, 4 (2015) 3–10, https://doi.org/10.1515/gps-2014-0095.
[30] F. Yang, F. Kubota, N. Kamiya, M. Goto, A comparative study of ionic liquids and a conventional organic solvent on the extraction of rare-earth ions with TOPO, Solvent Extract. Res. Dev. 20 (2013) 225–232, https://doi.org/10.15261/serdj.20.225.
[31] B.J. Rho, P.P. Sun, S.Y. Cho, Recovery of neodymium and praseodymium from nitrate-based leachate of permanent magnet by solvent extraction with trioctylphosphine oxide, Sep. Purif. Technol. 238 (2020), 116429, https://doi.org/10.1016/j.seppur.2019.116429.
[32] V. Dore, D. Tsaoulidis, P. Angeli, Mixing patterns in water plugs during water/ionic liquid segmented flow in microchannels, Chem. Eng. Sci. 80 (2012) 334–341, https://doi.org/10.1016/J.CES.2012.06.030.
[33] D. Tsaoulidis, M. Mamtora, M. Pineda, E.S. Fraga, P. Angeli, Experimental and CFD scale-up studies for intensified actinide/lanthanide separations, Chem. Eng. Process. - Process Intesif. 164 (2021), 108355, https://doi.org/10.1016/j.cep.2021.108355.
[34] P. Angeli, A. Gavriilidis, Hydrodynamics of Taylor flow in small channels: A Review. 222 (2008) 737–751. 10.1243/09544062JMES776.
[35] G. Balestra, L. Zhu, F. Gallaire, Viscous Taylor droplets in axisymmetric and planar tubes: from Bretherton's theory to empirical models, Microfluid Nanofluidics. 22 (2018) 67, https://doi.org/10.1007/s10404-018-2084-y.
[36] D. Tsaoulidis, P. Angeli, Effect of channel size on liquid-liquid plug flow in small channels, AIChE J 62 (2016) 315–324, https://doi.org/10.1002/AIC.15026.
[37] K. Takahashi, H. Takeuchi, Interfacial Area of Liquid-Liquid Dispersion in a Mixer-Settler Extraction Column, Process Metall. 7 (1992) 1357–1362, https://doi.org/10.1016/B978-0-444-88677-4.50043-X.